Developmental Biology 381 (2013) 377–388

Contents lists available at ScienceDirect

Developmental Biology

journal homepage: www.elsevier.com/locate/developmentalbiology

The zebrafish amyloid precursor protein-b is required for motor neuron guidance and synapse formation

Alexandra Abramsson [a,*], Petronella Kettunen [a], Rakesh K. Banote [a], Emelie Lott [a], Mei Li [b], Anders Arner [b], Henrik Zetterberg [a,c]

[a] Institute of Neuroscience and Physiology, Department of Psychiatry and Neurochemistry, The Sahlgrenska Academy, University of Gothenburg, S-41345 Gothenburg, Sweden
[b] Department of Physiology and Pharmacology, Karolinska Institutet, Stockholm, Sweden
[c] UCL Institute of Neurology, Queen Square, London WC1N 3BG, United Kingdom

ARTICLE INFO

Article history:
Received 11 January 2013
Received in revised form
26 June 2013
Accepted 27 June 2013
Available online 9 July 2013

Keywords:
Amyloid
Appb
Motor neuron
Development
Zebrafish
Locomotion

ABSTRACT

The amyloid precursor protein (APP) is a transmembrane protein mostly recognized for its association with Alzheimer's disease. The physiological function of APP is still not completely understood much because of the redundancy between genes in the APP family. In this study we have used zebrafish to study the physiological function of the zebrafish APP homologue, *appb*, during development. We show that *appb* is expressed in post-mitotic neurons in the spinal cord. Knockdown of *appb* by 50–60% results in a behavioral phenotype with increased spontaneous coiling and prolonged touch-induced activity. The spinal cord motor neurons in these embryos show defective formation and axonal outgrowth patterning. Reduction in Appb also results in patterning defects and changed density of pre- and post-synapses in the neuromuscular junctions. Together, our data show that development of functional locomotion in zebrafish depends on a critical role of Appb in the patterning of motor neurons and neuromuscular junctions.

Introduction

The amyloid precursor protein (APP) family members include the APP protein and the amyloid-beta precursor-like proteins (APLP) 1 and -2 which are ubiquitously expressed type I integral membrane proteins with relatively large extracellular and considerably smaller intracellular domains (Jacobsen and Iverfeldt, 2009). Although APP is expressed in many tissues, it is primarily recognized as a neuronal protein, enriched in the synapses of neurons and in peripheral tissues including the neuromuscular junctions (NMJ) of the skeletal muscle. Proteolytic processing of APP produces various fragments of which the amyloid-beta (Aβ) peptide aggregates to form plaques in the brains of patients with Alzheimer's disease (AD). Over the years, the role of APP in neurodegenerative diseases has been debated, however recent studies detecting changes in Aβ peptide level more than 10 years before the onset of AD, indicate a central function of APP in the AD pathogenesis (Bateman et al., 2012; Blennow et al., 2006; Buchhave et al., 2012; Pozueta et al., 2012). Thus, since APP still holds promise as a potential therapeutic target for AD an increased understanding of the physiological function of APP might reveal new mechanisms that can be used for future treatments.

APP has been suggested to function as a neurotrophic factor (LeBlanc et al., 1992; Perez et al., 1997) and to take part in neuronal migration (Young-Pearse et al., 2007), neurite outgrowth (Allinquant et al., 1995; Jin et al., 1994; Milward et al., 1992; Small et al., 1994), axon branching and pathfinding (Ikin et al., 2007), pruning (Nikolaev et al., 2009) and long-term potentiation (Dawson et al., 1999). Knockout studies in fruit fly and mice have also shown alterations in neuromuscular junctions (NMJs), as well as behavioral changes (Magara et al., 1999; Zheng et al., 1995). However, in vivo studies of the physiological function of APP in vertebrates are hampered by the redundancy between members of the APP family, especially with APLP2. In contrast, single knockout of the APP homologue Appb in zebrafish, results in embryonic lethality (Joshi et al., 2009), suggesting that the redundancy between Appb and Aplp2 is absent or weaker in zebrafish than in mice. The well-described development of spinal cord motor neurons and synapse formation in this model organism also make it suitable for the study of possible Appb functions in these processes (Devoto et al., 1996; Eisen, 1998; Westerfield and Eisen, 1988; Zeller et al., 2002).

In this study, we addressed the specific requirement of Appb for the development of motor neurons and for the formation of a

* Corresponding author. Fax: +46 31 828 458.
E-mail address: alexandra.abramsson@neuro.gu.se (A. Abramsson).

0012-1606/$ - see front matter © 2013 Elsevier Inc. All rights reserved.
http://dx.doi.org/10.1016/j.ydbio.2013.06.026

normal locomotor behavior. Zebrafish have two types of spinal motor neurons, primary motor neurons (PMNs) that are formed at late gastrulation and secondary motor neurons (SMNs) that are smaller and more numerous and formed slightly later. We found that Appb is required to sustain normal development of both primary and secondary motor neuron circuits and that a ~50–60% decrease in Appb expression results in changed locomotion behavior. The observed phenotype was not due to increased cell death in the spinal cord but seems to be the outcome of abnormal patterning, increased neurite branching and changed synaptic density. Our results not only support a role of Appb at the neuromuscular junction but also indicate that Appb is important during patterning of the projecting motor neuron axons. This provides evidence of an essential role of Appb during the neurogenesis of motor neurons and gives new insight into the physiological function of the APP family in vertebrates.

Materials and methods

Zebrafish maintenance

Zebrafish (*Danio rerio*) were kept at the Institute of Neuroscience and Physiology, University of Gothenburg, at a constant temperature of 28 °C and a 14:10-hour light:dark cycle. Embryos were raised at 28.5 °C. Wild-type fish and transgenic fish lines *Tg* (*CM-isl1:GFP)* (Higashijima et al., 2000), *Tg(mnx:GFP)* and *Tg*(*gata2:GFP*) (Meng et al., 1997) were of AB background. The study protocol was approved by the animal ethics committee of University of Gothenburg and followed the guidelines of the Swedish National Board for Laboratory Animals.

RT-PCR

The zebrafish *appb* cDNA was amplified using RT-PCR from 24 h post-fertilization (hpf) mRNA. RNA was collected from whole 24, 48 or 72 hpf embryos that had been injected with either the splice-blocking MO or a control MO using TRIzol reagent (Invitrogen, Carlsbad, US). cDNA synthesis was performed using oligo(dT) (GIBCO-BRL, Gaithersburg, MD) and Superscript III reverse transcriptase (RT; GIBCO-BRL, Gaithersburg, MD). PCR conditions were 5 min at 95 °C; 5 cycles at 95 °C for 1 min, 50 °C for 30 s, 72 °C for 30 s; 5 cycles at 95 °C for 1 min, 51 °C for 30 s, 72 °C for 30 s; 25 cycles at 95 °C for 1 min, 52 °C for 30 s, 72 °C for 30 s; followed by 72 °C for 7 min. The RT enzyme was omitted in the negative control. The sequence around exon 2 was amplified using primers in the first and third exon; fwd 5′-CGGAGCAGAAAATCGCGACAGAAA-3′ and rev 5′-GAACAACAATGTGCGTGTGACTGC-3′. PCR products were gel-purified and cloned (PCR-Script Cloning Kit, Stratagene, La Jolla, CA). M13 primers matching the cloning vector were used to amplify the cloned region, which was sequenced using the BigDye® Terminator v3.1 cycle sequencing kit (Applied Biosystems, Carlsbad, USA).

Morpholino oligonucleotides and mRNA injections

Morpholino oligonucleotide (MO) predicted to block the translation site of *appb* with the sequence 5′-TGTGTTCCCAAGCGCAGCACGTCCT-3′ (trlMO, binding nucleotide −4 to −28 from the ATG site) or splicing of exons 2 and 3 of *appb* with the sequence 5′-CTCTTTTCTCTCTCATTACCTCTTG-3′ (*appb*MO) was obtained from Gene-Tools (Philomath, OR). Both MOs gave the same phenotype at an equal dose; however the splice-blocking MO was used in all experiments except for the mRNA rescue. A standard control MO 5′- CCTCTTACCTCAGTTACAATTTATA-3′ was used as negative control (Gene-Tools). MOs were diluted in water and injected using borosilicate pipettes into one-cell wild-type embryos or embryos expressing the *Tg(isl1:GFP)*, *Tg(mnx1:GFP)* or the *Tg(gata2:GFP)*.

The effect of 2.5 ng splice-blocking MO on the RNA splicing was analyzed with PCR on cDNA from 24 hpf embryos injected with *appb*MO or control MO using primers binding to exon 1; 5′-TGCTGCGCTTGGGAACAC-3′, and a reverse primer in the third exon, 5′-GAACAACAATGTGCGTGTGACTGC-3′. Advantage 2 polymerase was used according to the manufacturer (Clontech Laboratories, Mountain View, CA).

The full length coding region of *appb* containing the 5′UTR region was amplified from cDNA prepared from AB embryos and inserted into the pCRII-TOPO vector (Clonetech Laboratories). A subclone of *appb* containing the Kozak sequence GCC (nucleotide-3 from the ATG site) upstream of the ATG site was subcloned into the pCDNA3 vector (Invitrogen). mRNA was synthesized from linearized DNA using the mMessage mMachine in vitro transcription kit (Invitrogen). The resulting mRNA lacks the 5′UTR upstream sequence recognized by the translation-blocking morpholino. mRNA and translation-blocking morpholino were diluted in water and injected into embryos at the one cell stage.

Whole-mount immunohistochemistry and in situ hybridization

Embryos at the specified stage were anesthetized using 0.02% tricaine methanesulfonate (MS-222) and fixed in 4% paraformaldehyde (PFA) as described (McGraw et al., 2008). Antibodies were used at the following concentrations: mouse znp1 (Developmental Studies Hybridoma Bank, DSHB) 1:500, mouse zn5 (DSHB) 1:1000, F59 (1:50, DSHB), 4D9 (1:50, DSHB), rabbit anti-GFP (Invitrogen) 1:1000, goat anti-mouse Alexa 488 (Invitrogen) and goat anti-rabbit Alexa 568 (Invitrogen) in blocking solution containing 2% goat serum. Acridine orange staining was done as previously described (Paquet et al., 2009). In short, live embryos were incubated in embryo medium containing 3 μg/ml acridine orange (Sigma-Aldrich) and 0.02% MS-222 for 30 min. Embryos were incubated in Phalloidin-Alexa568 (1:100, Invitrogen) in PBS with 2% TritonX-100 for 90 min to stain muscle F-actin. Embryos were cleared and mounted in 75% glycerol and imaged at the Centre for Cellular Imaging, the Sahlgrenska Academy, with a Zeiss LSM 710.

RNA in situ hybridization was performed as described before (Andermann et al., 2002). In brief digoxigenin-labeled antisense probe was generated from cDNA for the full length *appb*. Hybridization was performed at 70 °C and probe-binding was visualized using NBT/BCIP (Roche). Embryos were stored in 50% glycerol/PBS for imaging using a Zeiss Axio Scope A1.

Behavior analyses

Spontaneous activity and swimming behavior was monitored using the ZebraLab system (Viewpoint Life Sciences, France). Fish were de-chorionated, staged for equal developmental stage and kept one and one in a 24-well cell culture plate containing embryo medium during the experiment (12 embryos injected with control morpholino and 12 embryos with *appb* morpholino). Monitoring was performed at constant light (100%) and temperature (28 °C). Activity was measured in tracking mode and the integration time was 60 s. The movement thresholds were set to inactivity <2 mm/s, small activity 2–4 mm/s, large activity >4 mm/s. Data analysis was made in Microsoft Excel and diagrams and statistical analysis using two-way ANOVA test was performed in GraphPad Prism version 6.00 for Windows (GraphPad Software, La Jolla CA, USA).

The startle response was measured in 3 dpf larval animals embedded in 1.7% low-melting point agarose (Invitrogen) in a small chamber. After embedding, agarose from the tip of the tail was gently removed liberating the tail. The startle response was

elicited by weak electrical stimulations delivered to the skin via a thin bipolar tungsten electrode. One pole of the electrode lightly touched the skin on the head of the fish, and the other pole was placed in the agar <0.5 mm away (Supplementary movie 1). The electrode was coupled to a 2100 isolated pulse stimulator (A-M Systems Inc., Sequim, WA) eliciting pulses, normally ranging between 6 and 9 V. The intensity of the stimulus pulses, which was determined prior to an experiment, was set to the threshold voltage for eliciting movement of the tail. A Photon Fastcam high-speed CCD camera (San Diego, CA) was used to capture short movies at 1000 frames/s to analyze the duration of the tail flips. The movies of tail movements were visualized using VirtualDub 1.9.11 Software. Statistical significance of differences in tail movement duration between all groups was calculated using Kruskal–Wallis Test. Mann–Whitney U Test was used for comparison between two treatments. *P*-values less than 0.05 were considered significant. Statistical analysis was made in SPSS.

Muscle physiology

To analyze the mechanical properties of the skeletal muscles, control- and MO-injected larvae (4 dpf) were mounted for force-recording as described previously (Dou et al., 2008). In short, the larvae were killed and mounted using aluminum clips between a fixed hook and a force transducer on a micrometer screw for length adjustment. The preparations were held in a bicarbonate buffered salt solution at 22 °C and stimulated via two platinum electrodes using 0.5 ms pulses at optimal voltage at 2 min intervals to give single twitches. The optimal length for active force was determined and the contraction at this length was taken as the maximal active force of the preparation. Muscles were also stimulated at optimal length using different pulse durations (0.01–0.5 ms) to determine the excitability of the neuromuscular activation pathway.

Synapse quantification

Quantification of pre- and post-synapses were made on confocal stacks using the Volocity® 3D Image Analysis Software 6.0.1 (Perkin Elmer, US). Data analyses were made in Microsoft Excel and GraphPad Prism version 6.00 for Windows (La Jolla CA, USA).

Results

Partial knockdown of zebrafish appb

The zebrafish APP homologue, Appb, has been shown to be essential for the convergence-extension process during early development (Joshi et al., 2009). Since a complete lack of Appb is embryonic lethal, we set out to find a morpholino dose that would enable a normal gastrulation process and thus allow studies of the subsequent neurogenesis. For this we used two different morpholinos, one blocking the donor site of exon 2 (appbMO) and the other blocking the translation initiation site (trslMO) upstream of the ATG site. Injection of 2.5 ng of morpholino resulted in embryos with slightly delayed development and a transient undulation of the notochord by 24 hpf (Fig. 1A–D). We observed that cells within the notochord had a rounder shape in morpholino-injected embryos compared to staged controls (Fig. 1E and F). A similar notochord phenotype has been described in embryos with mutations in genes involved in both structure and signaling (Stemple et al., 1996) but may also depend on abnormal muscle contractions (Teraoka et al., 2006). The *appb* morphants ($n=15$) were also slightly shorter than their staged controls ($n=15$) and had an increased somite-to-midline angle as a result of reduced somite width in the anterior to posterior axis (Fig. 2A,C, D) which could be rescued by co-injecting *trsl*MO+*appb* mRNA ($n=15$, Fig. 2A,C,D). The notochord phenotype of *appb* morphants was more apparent during spontaneous contractions indicating

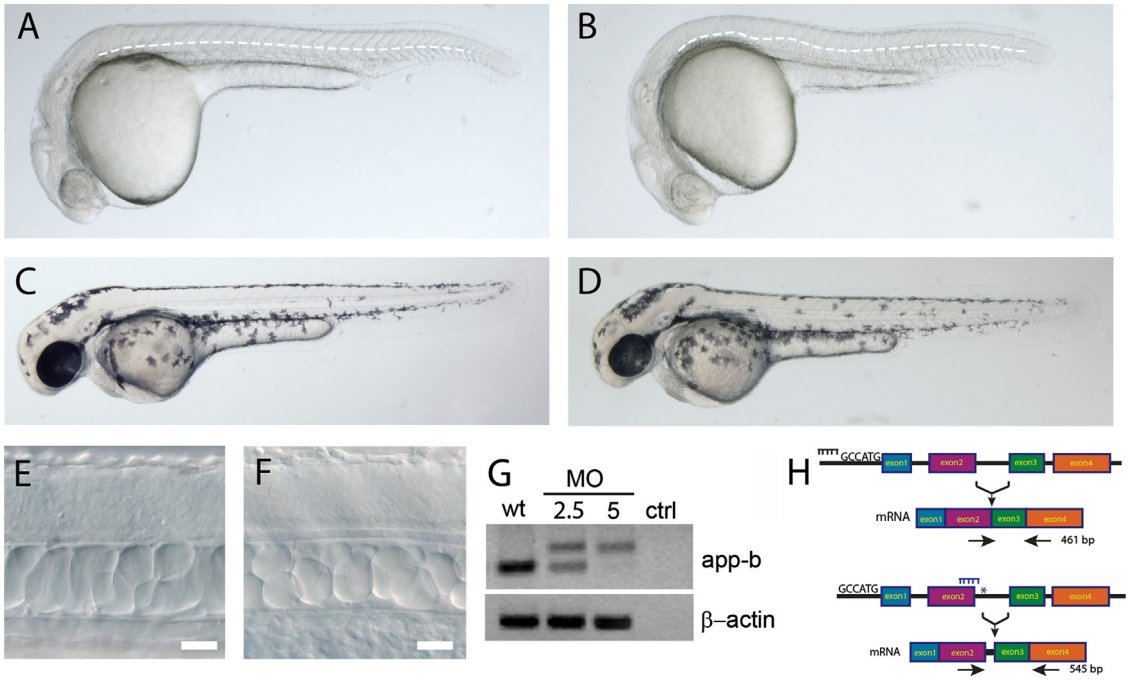

Fig. 1. Partial knock-down of *appb*. Injection of 2.5 ng morpholino (MO) designed against *appb* results in an undulating notochord (B, dashed line) not present in animals injected with control MO at 24 hpf (A). Otherwise, the gross morphology of embryos injected with control (C) or *appb* morpholino (D) is comparable at 48 hpf. Cells within the notochord of *appb* morphants (F) are less vacuolated compared to controls (E). RT-PCR amplification of exon 1 and 4 (G,H) results in a larger fragment in embryos injected with *appb* morpholino than control morpholino (G). At 2.5 ng approximately 50–60% of the wildtype transcript was present, whereas it was absent at 5 ng morpholino. (H) Schematic illustration of wildtype and trslMO splicing (upper) and the effect of the *appb* morpholino (blue comb) on splicing. Blocking the splicing of intron 2 activates an alternative splice site (∗) within intron 2 resulting in a premature stop in exon 3 (H). Scale bar: 20 μm.

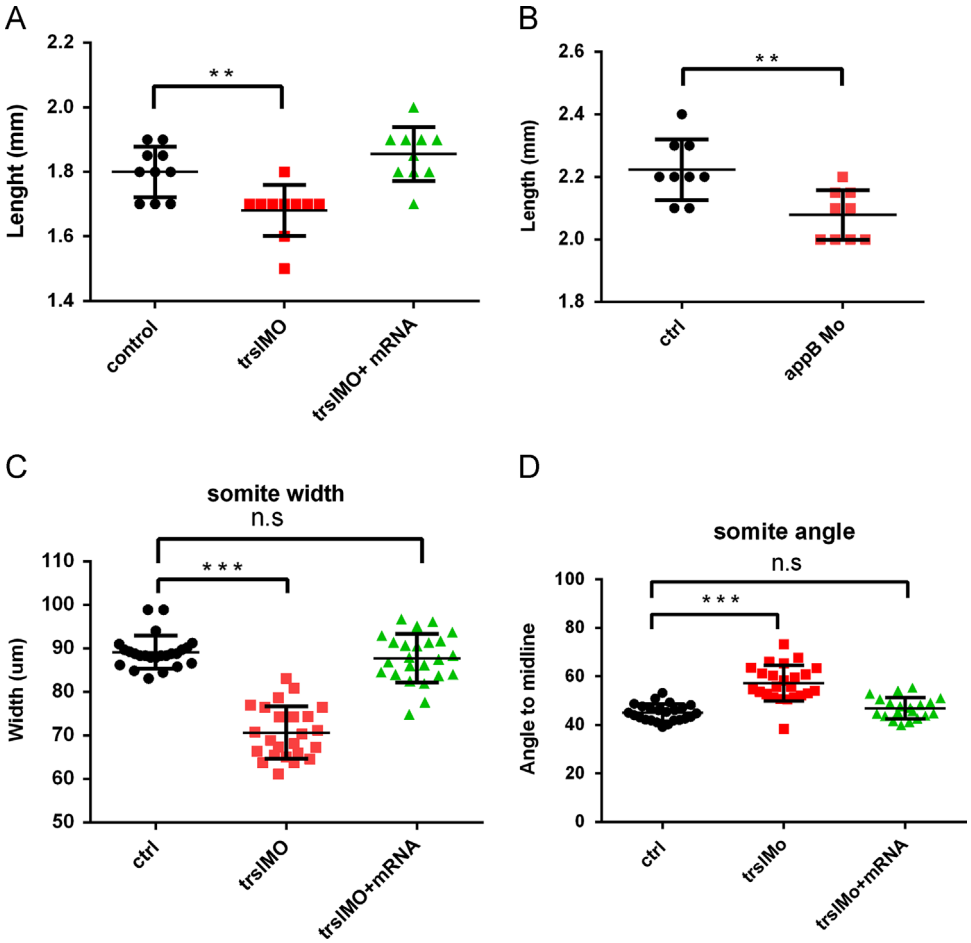

Fig. 2. Changed body length and somite properties of embryos injected with trslMO or trslMO+mRNA. The average length of control ($n=10$), *trsl*MO ($n=10$) and *trsl*MO +mRNA ($n=10$) injected embryos at 24 hpf in embryo medium (A). Average length of control ($n=10$) and *appb*MO ($n=10$) embryos incubated with 0.02% MS-222 for 60 min (B). Measurement of the anterior to posterior somite width (C) and the somite-boundary to-midline-angle (C). Two-way ANOVA test: $^{***}P<0.0005$, $^{**}P<0.05$.

that the waviness was exacerbated upon muscle contraction. To address if the wavy notochord and shorter body phenotypes were due to increased muscular tonus we treated embryos with tricaine, a weak Na+ channel inhibitor, to relax muscles. Incubation with 0.02% tricaine for 60 min eliminated the waviness of the notochord of *trslMO* -injected embryos ($n=10$) but did not have any substantial effect on the body length as compared to control injected embryos ($n=10$, Fig. 2B). This suggests that the wavy notochord was not the result of increased muscular tonus but rather an effect of impaired notochord development.

RT-PCR on embryos injected with 2.5 ng morpholino demonstrating a wavy notochord at 24 hpf showed an alternative splicing and reduction of the wildtype fragment with approximately 50% (Fig. 1G). In embryos injected with 5 ng, resulting in a lethal phenotype, all wildtype transcripts were lost and only the splice-interfered larger transcript was present (Fig. 1G). Hence, injection of 2.5 ng *appb*MO gave rise to a morphant equivalent to a viable heterozygous mutant and was the dose used from here on. Cloning and sequencing of the amplified transcript from 24 hpf embryos injected with control or *appb*MO revealed that activation of a cryptic splice site within the second intron introduced a premature stop codon most likely resulting in protein degradation (Fig. 1G and H). Both the translational and splice-blocking morpholino resulted in a similar phenotype in a dose-dependent manner. However, the latter was preferably used since it gave us the opportunity to control for the morpholino effect on the transcriptional level.

Table 1
mRNA rescue of the appb morpholino phenotype.

Genotype	**Normal NC**	**Wavy NC**	**Normal NC (%)**
Control MO ($n=51$)	51	0	100
trslMO 2.5 ng *($n=51$)*	6	45	13
trslMO+appb mRNA ($n=35$)	28	7	75

To confirm that the phenotype was *appb*-specific we injected the *trslMO* together with mRNA encoding the zebrafish $Appb_{694}$ lacking the upstream sequence recognized by the morpholino (nucleotide −4 from the ATG). Fifty pg *appb* mRNA encoding the $Appb_{694}$ rescued the notochord phenotype in 85% of the injected embryos (Table 1). This, in combination with the finding that the two morpholinos gave rise to the same phenotype and that the phenotype was more severe when less wildtype transcript was present, strongly indicates that the phenotype observed is specific to a decrease in Appb.

Hyperactivity in appb morphants

Morpholino-injected embryos could, in addition to the wavy notochord, be distinguished from control embryos by their increased locomotion. The sequential and stereotypic behaviors that the zebrafish embryo passes through during development have been described as an initial period of extensive spontaneous coiling contractions starting at 17 hpf that is followed

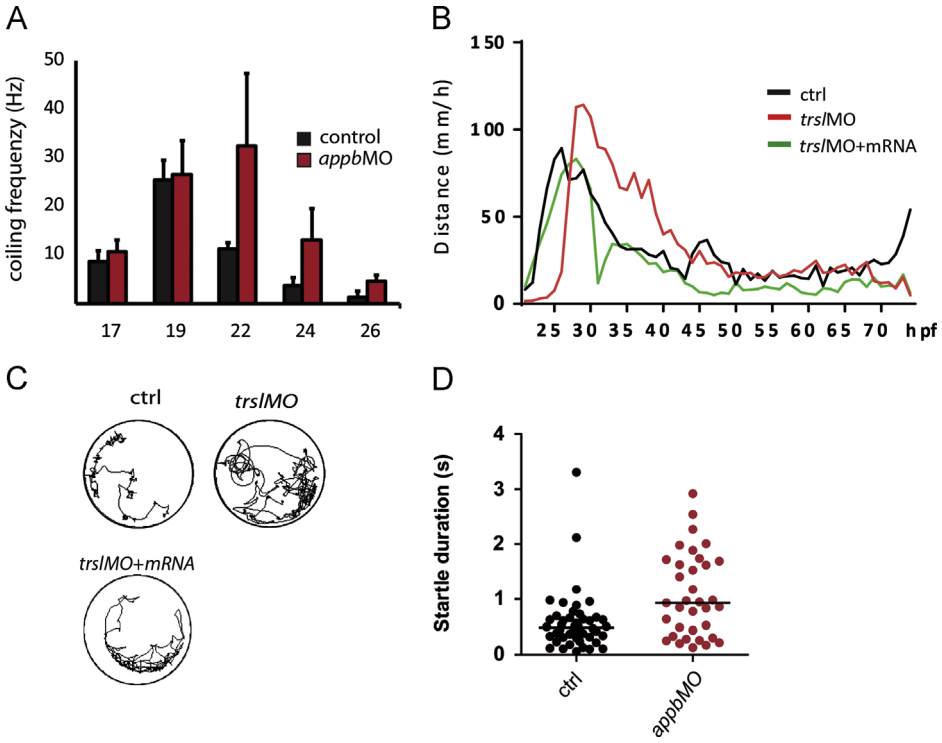

Fig. 3. Locomotor behavior defects. Frequency of spontaneous coiling in *appb* morpholino ($n=20$, red) injected embryos and control ($n=20$, black) between 17 and 26 hpf (A). Total distance during spontaneous movement of embryos injected with control (black), *trsl*MO (red) and *trsl*MO+mRNA (green) between 22 and 72 hpf(B). Representative plot of movement (C). Startle duration of *appb*MO ($n=15$) and control MO ($n=20$) injected embryos at 3 dpf (D).

by touch-evoked rapid coils by 21 hpf and finally organized into swimming after 26 hpf (Brustein et al., 2003; Saint-Amant and Drapeau, 1998). We measured the activity of embryos injected with *appb* or control morpholino simply by counting the number of tail beats per minute at different time points during the early development stages (Fig. 3A). We found that the spontaneous tail flips initiated at 17 hpf in both *appb* morphants and controls but that *appb* morphants exhibited a more than 3-fold increased activity by 24 hpf (Fig. 3A). Although the spontaneous coiling decreased over time, *appb* morphants still moved more than 3 times as much as controls by 26 hpf (Fig. 3A).

To address whether the swimming behavior emerging around 26 hpf was affected, we video-tracked the activity of controls and *appb* morphants between 24 and 72 hpf. Since body shape (e.g. curvature) is likely to affect swimming, only fish with a mild notochord phenotype were used. The total distance moved was increased between 28 and 45 hpf in morphants ($n=22$) compared to controls ($n=35$) (Fig. 3B and C). Co-injections of *trslMO* and *appb* mRNA rescued the increased locomotion phenotype (Fig. 3B and C). To rule out that the change in behavior resulted from general cell death in the spinal cord, embryos at 2 dpf were stained with acridine orange that binds to DNA in dying cells and can be used to measure cell death in living embryos (Furutani-Seiki et al., 1996). No significant difference in cell death was found in the spinal cord of larvae injected with 2.5 ng *appb* morpholino versus control morpholino (data not shown).

Finally, the touch-induced response was analyzed by mounting embryos in agarose leaving their tail free and stimulated them with a short electrical pulse at the head region. The duration of the subsequent tail flips were measured and compared between control- and *appbMO*-injected embryos. Similar to the spontaneous movements, we observed an increased tail flip duration in *appbMO*-injected embryos (Fig. 3D). Although the inter-individual variability in morphants was high, there was a significant increase in the response duration in larvae injected with the *appb* morpholino (1.69 s $\pm$ 0.54) compared to control (0.51 s $\pm$ 0.14) injected embryos (Fig. 3D and Supplementary Movie 1 A,B). Together, this shows that Appb is essential for the development of normal locomotion and that the lack of Appb results in increased spontaneous as well as prolonged touch-induced locomotion.

Supplementary material related to this article can be found online at http://dx.doi.org/10.1016/j.ydbio.2013.06.026.

Expression of appb in motor neurons

Our results show that Appb is important for the development of normal behavior in zebrafish although the function of the skeletal musculature per se seems to be conserved. To better understand the role of Appb we therefore continued by examining its cell-specific expression in the tail during development. We found strong expression of *appb* in axial structures during gastrulation and in the spinal cord up to 48 hpf (Fig. 4). By 48 hpf, *appb* expression is strong in the head region but was weak or absent in the spinal (Fig. 4 and Musa et al., 2001). Cross sections of embryos at 24 hpf showed a pronounced expression of *appb* in post-mitotic neurons while immature neurons located closer to the center of the spinal cord did not express *appb* (Fig. 4). The subsequent down-regulation of *appb* in the spinal cord suggests a requirement of Appb during the initial development and establishment of these neurons.

Defects in PMN axon outgrowth

The expression pattern of *appb* in the spinal cord and the changed locomotor activity observed in embryos with decreased Appb levels, prompted us to look closer on the developing motor neurons. Zebrafish have three types of PMNs, the caudal primary (CaP), middle primary (MiP) and rostral primary (RoP) neurons that develop in the ventromedial part of the spinal cord and project axons to specific muscle territories of the embryo (Beattie,

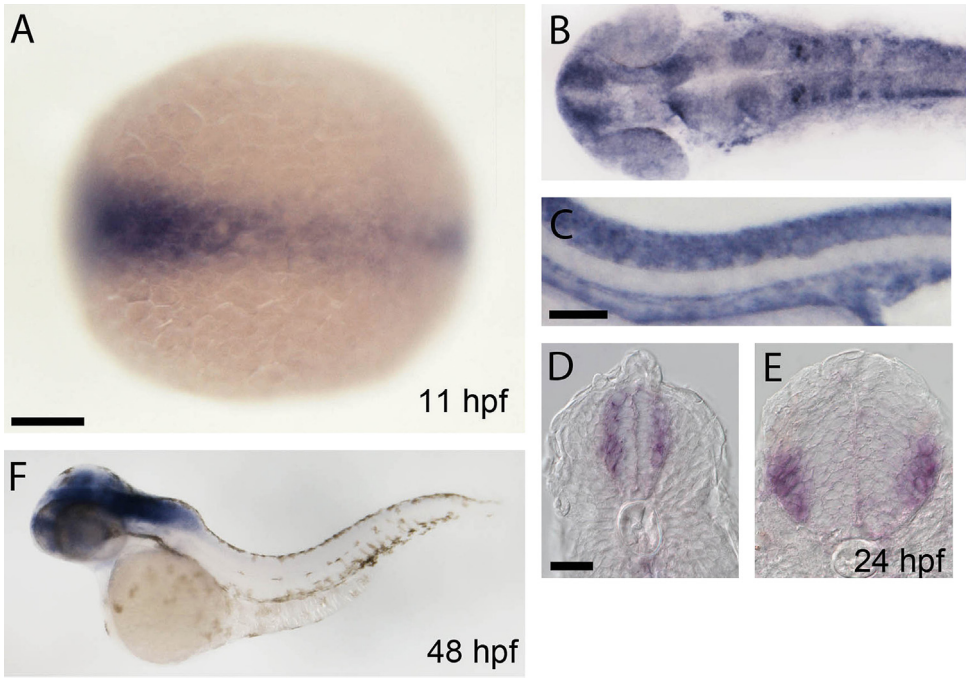

Fig. 4. Expression of *appb* at 11, 24 and 48 hpf. The expression of *appb* is prominent in axial structures at 11 hpf (A) and is expressed in telencephalon, spinal cord neurons and pronephric duct and dorsal aorta by 24 hpf (B,C). Cross section at the caudal hindbrain and spinal cord shows expression in developing motor neurons and interneurons (D,E). The expression of *appb* becomes restricted to CNS at 48 hpf, (F). Scale bars: A, 100 μm; C, 80 μm; D, 40 μm.

2000; Myers et al., 1986; Westerfield et al., 1986). We partially knocked down *appb* in the *Tg*(*mnx1:GFP*) fish line expressing GFP under the *hb9*-promoter in both somas and peripheral axons of PMNs and interneurons (Flanagan-Steet et al., 2005). At 24 hpf the CaP axons were shorter and occasionally missing in *appb* morphants (compared to controls (Fig. 5A and B). This phenotype was rescued by co-injecting 50 pg of mRNA coding for the *appb* gene (Fig. 5C). The outgrowth of the MiP axons was also slightly shorter in the *appb* knockdown embryos but not significantly different as compared to controls (Fig. 5G and H). Quantification of the length of CaP and MiP in ten segments of equally staged embryos showed that the ventral axon of the CaP were significant shorter in *appb* morphants ($n=20$) as compared to controls ($n=20$) and rescued ($n=20$) embryos (Fig. 5G). There was also a tendency towards shorter MiP axons in *appb* morphants (5H). In addition, while approximately 8.3% of all axons in *appb* morphants ($n=30$) stalled at or before the horizontal myoseptum only 0.61% stalled in controls ($n=29$, Table 2). Analysis of mRNA rescued embryos ($n=18$) showed that this phenotype was restored (0.24%, Table 2). The amount of branching at 24 hpf was measured as the number of branches from the CaP axon. While 15.5% of axons in control injected embryos had 2–3 branches, *appb* morphants had increased number axons with 3–5 branches (2.53%) while less of 2–3 branches (10.8%, Table 2). Thus, it seems as if motor neurons projecting ventrally are more affected by changes in Appb levels. Embryos were co-labeled with the PMN-specific znp1 antibody to rule out that the CaP axons were present but not expressing GFP. This showed a similar CaP outgrowth as the *Tg*(*mnx1:GFP*) fish line (Fig. 5D and F).

Mis-patterning of SMNs

The secondary motor neurons follow the same paths as PMN and migrate through the common path and then sprout into the ventral or dorsal myotome (Myers, 1985; Myers et al., 1986; Westerfield et al., 1986). Knockdown of *appb* in *Tg*(*isl1:GFP*) fish expressing GFP in SMN projecting axons dorsal or at the horizontal myoseptum (Higashijima et al., 2000) was reported to result in a strong down-regulation of GFP expression in the spinal cord (Song and Pimplikar, 2012). We repeated their experimental setup and confirmed that the GFP expression in the spinal cord was reduced in embryos injected with the *appb* morpholino (Fig. 6A and B). Since the *Tg*(*isl1:GFP*) fish (Higashijima et al., 2000) does not express GFP in ventrally projecting neurons, embryos were double-labeled with the zn5 antibody to mark the ventral axons of the SMNs. We were surprised to find that both dorsal and ventral projections were present in the *appb* morphants (Fig. 6A and B). Motor neuron axons project out from the spinal cord at pre-defined exit points and follow migration cues from the surrounding tissue to form a highly stereotypic pattern (Kucenas et al., 2009). However, in the *appb* morphants, we observed additional protrusions from the spinal cord giving rise to an irregular pattern of SMN axons (Fig. 6B, arrowhead). A similar phenotype was observed at 48–72 hpf in *Tg(gata2:GFP)* embryos expressing GFP in ventrally projecting SMNs (Fig. 6C and D). Together these findings suggest that Appb is involved in patterning of the projecting axons and may also have a role during differentiation of spinal cord neurons.

Normal muscle physiology in Appb morphants

Swimming in fish is composed of complex neural circuits in the brain and spinal cord conveying information from sensory neurons to muscle fibers (Berkowitz et al., 2010; Brownstone and Bui, 2010; Fetcho et al., 2008; Gabriel et al., 2011; Goulding, 2009; Grillner and Jessell, 2009). APP is ubiquitously expressed including both muscle and neurons and plays an important role during the formation of NMJ in mouse skeletal muscle (Wang et al., 2005; Wang et al., 2009). To examine if the locomotion changes in *appb* morphants were caused by alterations in skeletal muscle function, we first determined the maximum active force in skeletal muscle. We did not detect any morphant-specific changes (Supplementary Fig. S1A). However, when the dependence of force on pulse duration was examined (Supplementary Fig. S1B),

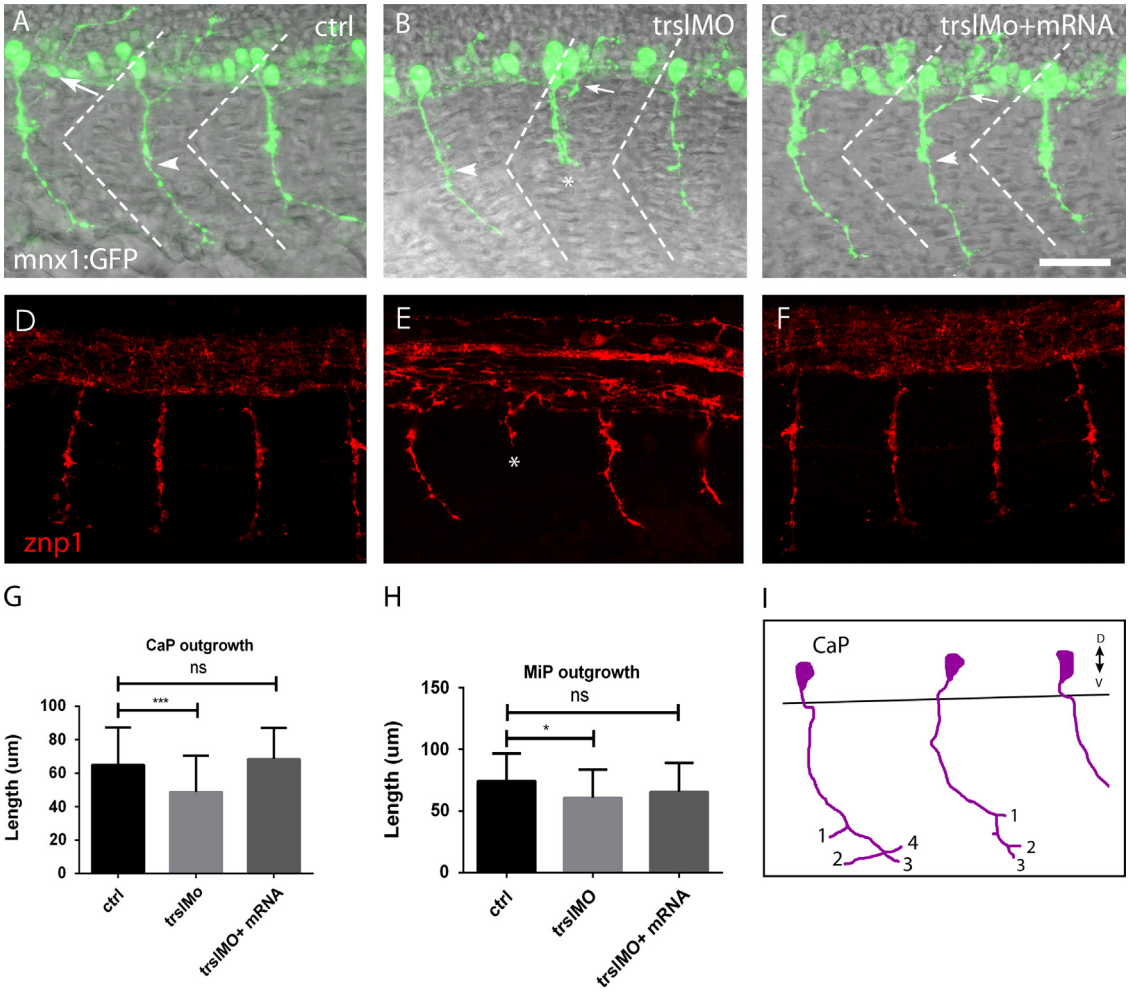

Fig. 5. Defective primary motor neurons. PMNs in the spinal cord of control embryos (A), *trsl*MO (B) and *trsl*MO +mRNA (C) injected *Tg(mnx1:GFP)* embryos (B) have dorsally projecting MiPs (arrow) and ventrally projecting CaP (arrowhead). Staining of control (D), *trsl*MO (E) and *trsl*MO +mRNA (F) injected embryos using znp1. CaP neurons stalling was observed in trslMO injected embryos (*). Measurement of the length of CaP (G) and MiP (H). Bar is 20 μm. Two-way ANOVA test: $^{***}P < 0.0005$, $^{*}P < 0.05$, n.s.= not significant.

Table 2
Summary of CaP motor neuron phenotype at 24 hpf.

Genotype	***n* (# of axons)**	**Stalled axons (%)[a]**	**2 Branches (%)**	**3 Branches (%)**	**4 Branches (%)**	**5 Branches (%)**
Control MO (n=29)	658	0.61	11.40	4.1	0.15	0
trslMO 2.5 ng *(n=30)*	672	8.63	7.29	3.57	1.74	0.79
trslMO+appb mRNA (n=18)	415	0.24	NA	NA	NA	NA

[a] Stalled axons measure CaP axons > 30% shorter than the average CaP axon of control embryos.

we observed a tendency to increased muscle responses at lower pulse durations (considered to activate motor neurons and muscle cells with lower threshold) in *appb* morphants. This is consistent with a hyper-excitability in the motor neuronal compartment, possibly a contributing component to the altered locomotion pattern.

We also investigated the effect of *appb* on the differentiation of the axial musculature by immunostaining with antibody F59, that predominantly recognizes slow muscle myosin fibers (Behra et al., 2002), and phalloidin that specifically recognizes F-actin of fast muscle fibers. We could not find any gross change in the formation or morphology of the developing muscle in *appb* morphants ($n=20$) as compared to controls ($n=23$, Fig. 7). Together these findings suggest that a partial knockdown of *appb* does not have a major effect on muscle development or physiology.

Changed pre- and post-synaptic density

To form a functional muscular unit, motor neurons grow out from the spinal cord to establish contact with muscle fibers of the corresponding somite. The importance of signaling between nerve and muscle in promoting proper synapse formation is well documented (Sanes and Lichtman, 1999). Interestingly, studies have shown that APP is needed both in motor neuron and in the post-synaptic motor neuron junctions located in the muscle fibers to form normally patterned pre- and post-synapses (Wang et al., 2005, 2009). This encouraged us to address if the error-prone axonal projection also is associated with an abnormal NMJ pattern. Embryos between 24 and 72 hpf were therefore co-stained with SV2 antibody marking the pre-synaptic motor nerve ends and α-bungarotoxin, binding to the post-synaptic acetylcholine receptors, AChRs. High resolution

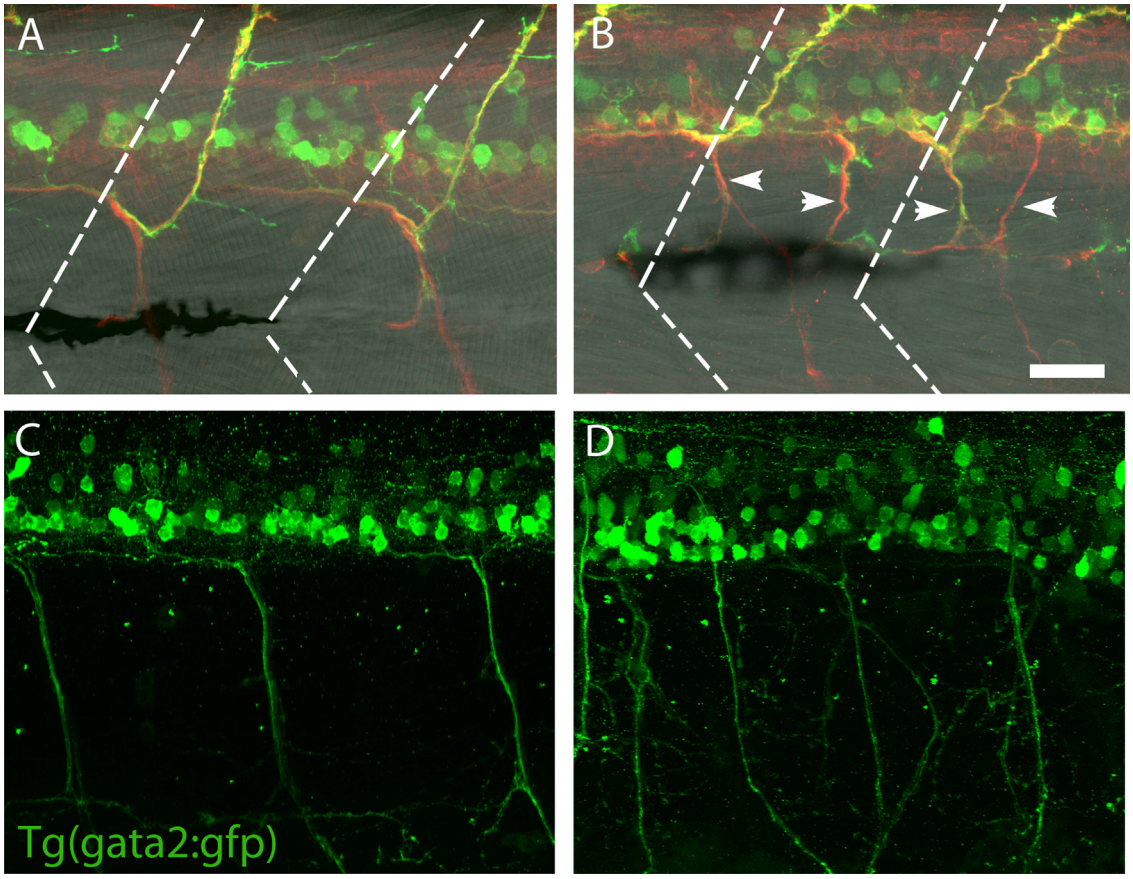

Fig. 6. Impaired patterning of the secondary motor neurons. The Tg(*isl1*:GFP) is expressed in SMNs of controls (A) but is reduced in *appb*MO injected embryos (B). Staining with the SMN-specific antibody zn5 shows irregular projections and stalled outgrowth of the SMN in *appb* morpholino injected embryos (B) compared to controls (A). The Tg (*gata2*:*GFP*) transgene shows that the irregular patterning of extending axons persist in morphants (D) while controls (C) have a regular pattern of SMN by 3 dpf. The dorsolateral fasciculus (DLF) which extends to the end of the spinal cord in controls (E) is projecting out to the tip of the tail fin in *appb* morphants (arrow, F). The contour of the tail fin is outlined by a dotted line. Bar: 20 μm.

confocal images were acquired from dorsal, ventral and midline projections of two adjacent somites of each animal (Fig. 8). Quantification of the pre- and post-synaptic densities at 3 dpf showed that *appb* morphants had lower density of post-synapses and increased density of pre-synapses as compared with controls (Fig. 8). The most significant difference was found at the horizontal myoseptum (Fig. 8). We also observed a strong reduction of the post-synaptic density at the somitic borders. This pre-synaptic increase matches the excessive branching of motor neurons in the morphants.

Axonal extension by the nascent motor neuron axon towards its muscular target depends on a wide variety of mechanisms governed by attraction and repulsion cues in the surrounding tissue. It has been shown that the NMJs are pre-patterned long before innervation but still seem to be involved in the guidance of outgrowing motor neurons (Flanagan-Steet et al., 2005; Panzer et al., 2005). This made us ask if Appb affects the NMJ pattern. As previously described, pre-formed NMJs were found in contact with or ahead of the sprouting nerve tip in both controls and *appb* morphants. However, at later time points the ventral growing neuron had axon sprouts neither touching nor migrating towards a pre-formed post-synaptic junction (Fig. 9A and B). Thus, if the pre-formed AChR clusters are important to guide the MN axon down its ventral track their loss might explain the excessive abnormal motor neuron morphology in *appb* morphants (Fig. 8A and B). While these pre-formed AChR clusters are formed before the motor neurons reach them they also disappear if the motor neurons do not target them. An alternative explanation might therefore be that NMJs disappear as the motor neuron outgrowth is delayed.

Discussion

The outgrowth of motor neurons is spatially restricted and orchestrated by the surrounding tissue to form an iterated pattern of neuromuscular connections in each somite. Here we show that *appb,* a highly conserved homologue to the human APP, has a crucial function for the outgrowth and synapse formation of motor neurons in the zebrafish. The neuronal defects are manifested as increased spontaneous activity during early development, followed by abnormal swimming behavior. There is accumulating evidence that disturbances in APP give rise to motor pathology in humans, mice and fruit fly (Kim et al., 2011; Seo et al., 2010; Lalonde et al., 2012). However, to our knowledge, our data provide the first in vivo evidence of a role of APP in guiding spinal cord motor neurons during axogenesis.

Behavior defects in Appb morphants

In mice, members of the APP family have redundant gene function making studies of the individual genes difficult to interpret, since several APP members need to be down regulated to generate an apparent phenotype (Heber et al., 2000). In contrast, knocking down one of the zebrafish APP homologue Appb, results in severe developmental defects in the convergence-extension process during gastrulation and embryonic lethality (Joshi et al., 2009). The strict requirement of Appb during early development has obscured studies of processes during neurogenesis. However, by partial knockdown creating a hypomorph, we found that Appb is required for the formation of a normal locomotor behavior.

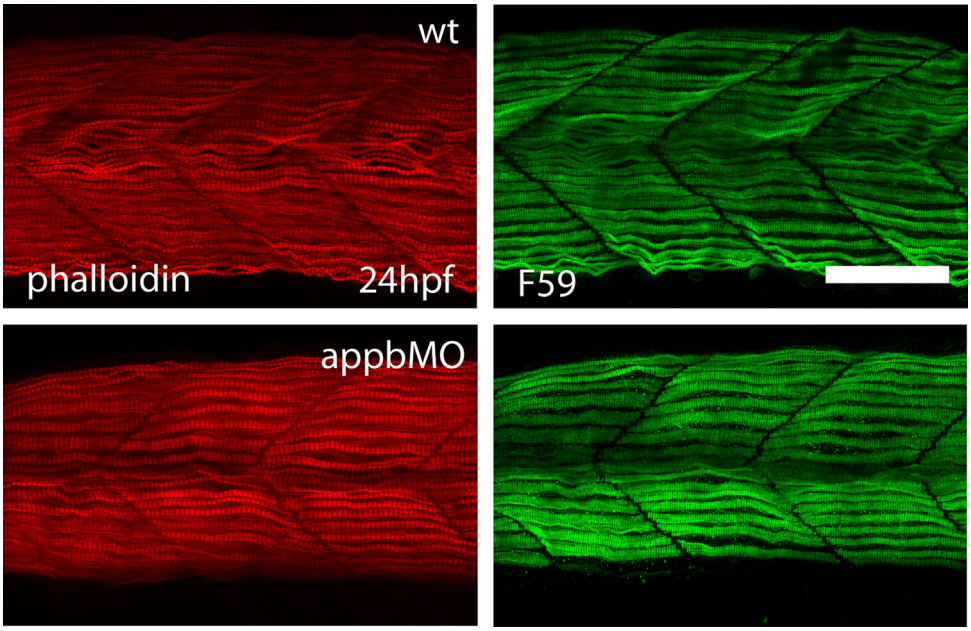

Fig. 7. No change in the development of slow and fast muscle fibers. Staining of fast muscle fibers with phalloidin (A,C) and slow muscle fibers with F59 (B,D) does not reveal differences in muscle morphology or differentiation between control ($n=20$, A,B) and *appb*MO ($n=23$, C,D) injected fish. Scale bar is 20 μm.

This adds to a growing list of genes with neuromuscular implications. However, unlike most genes identified in this group, we found that even a 50–60% decrease in Appb had profound effects on locomotion. The observed rescue of behavioral and morphological phenotypes of Appb knockdown by co-injections with mRNA coding for Appb argues for a specific effect of the *appb* morpholino.

The undulating notochord, which is typical for the *appb* morphants, has been described in several other motor neural mutants (Hirata et al., 2009). Although these mutations affect genes functioning in muscle, neurons or the transmission in between these, they all lead to very similar phenotypes. The waviness of the notochord in Appb morphants is likely to result from muscle contractions since treatment of embryos with the muscle relaxing agent tricaine restores the notochord phenotype. However, the length of the embryos could not be restored by relaxing muscle. In combination with the functionally normal muscle physiology, this argues that the notochord defect primarily is structural and not secondary to a muscle contraction defect. This supports a role for Appb during gastrulation and development of the notochord (Joshi et al., 2009).

The significant increase in coiling started at 21 hpf, a time point when the behavior is unaffected by the brain and only depends on signals from the spinal cord (Saint-Amant and Drapeau, 1998). We show that this hyperactivity is not caused by defective or delayed muscle development since the initial coiling contractions, which are spontaneous muscle contractions, develop concurrently in both controls and *appb* morphants. Although the activity continued to be higher even as the spontaneous movements developed into swimming it slowly decreased to reach that of controls by 48 hpf. At 3 dpf the duration of the touch-induced response was extended in Appb morphants. These findings suggest a function of Appb in the formation of a functional neural network in the spinal cord or in the synaptic junctions with muscle fibers, which was further supported by the normal muscle physiology tests. It is well known that changes in APP or its cleavage result in behavioral abnormalities. Contrary to our findings, mice lacking APP have decreased locomotor activity and grip strength (Dawson et al., 1999) while mice carrying double mutations in App and Presenillin-1 (APP/PS1) show increased activity (Holcomb et al., 1999).

Although the hyperactivity that we observed in zebrafish declines by age, behavioral analysis after 4 dpf was hampered due to the reduced effects of the morpholino. Hence, at present we are not able to address the full consequence of reduced Appb levels in zebrafish. Nonetheless, our behavioral tests highlight the importance of Appb for the formation of normal locomotion and indicate that it is confined to the motor neuron circuitry in the spinal cord since defects are present already before the involvement of the higher brain structures. The sensitivity to changes in Appb level might reflect that the ancient genome duplication in teleosts, giving rise to two APP homologues, has resulted in gene specification possibly making the function more specific (Musa et al., 2001). This might also explain why Appb has not been identified in earlier screens for motor neural mutants. Further studies are needed to fully understand the role of Appb in locomotion. However, since other App family members do not seem to be redundant with Appb, zebrafish might be the model of choice.

Defective motor neuron outgrowth and synapse formation

The behavioral analysis strongly indicated a role of Appb in the formation of a motor neural circuit. Imaging of the developing PMNs in the *appb* hypomorphs revealed shorter axonal outgrowth combined with increased arborization of the PMNs pioneering the ventral pathway. Although axons of the PMNs generally migrate on the common path in the midsection of each somite and eventually seem to reach their ventral targets, they form excessive branches. Our results also indicate that while the outgrowth of the ventrally projecting CaP axons are shorter or stalled by a decrease in Appb the dorsally projecting MiP axons are only slightly affected. In zebrafish, PMNs elicit spontaneous activity as they are navigated to their targets (Milner and Landmesser, 1999). These bursts decrease over time as the PMNs mature and establish NMJs. This decrease coincides with the initiation of the spontaneous contractions observed at 17 hpf. Hence, it is attractive to speculate that the stalled axons might give rise to spontaneous bursts over a longer period of time giving rise to the prolonged activity observed between 21 and 26 hpf.

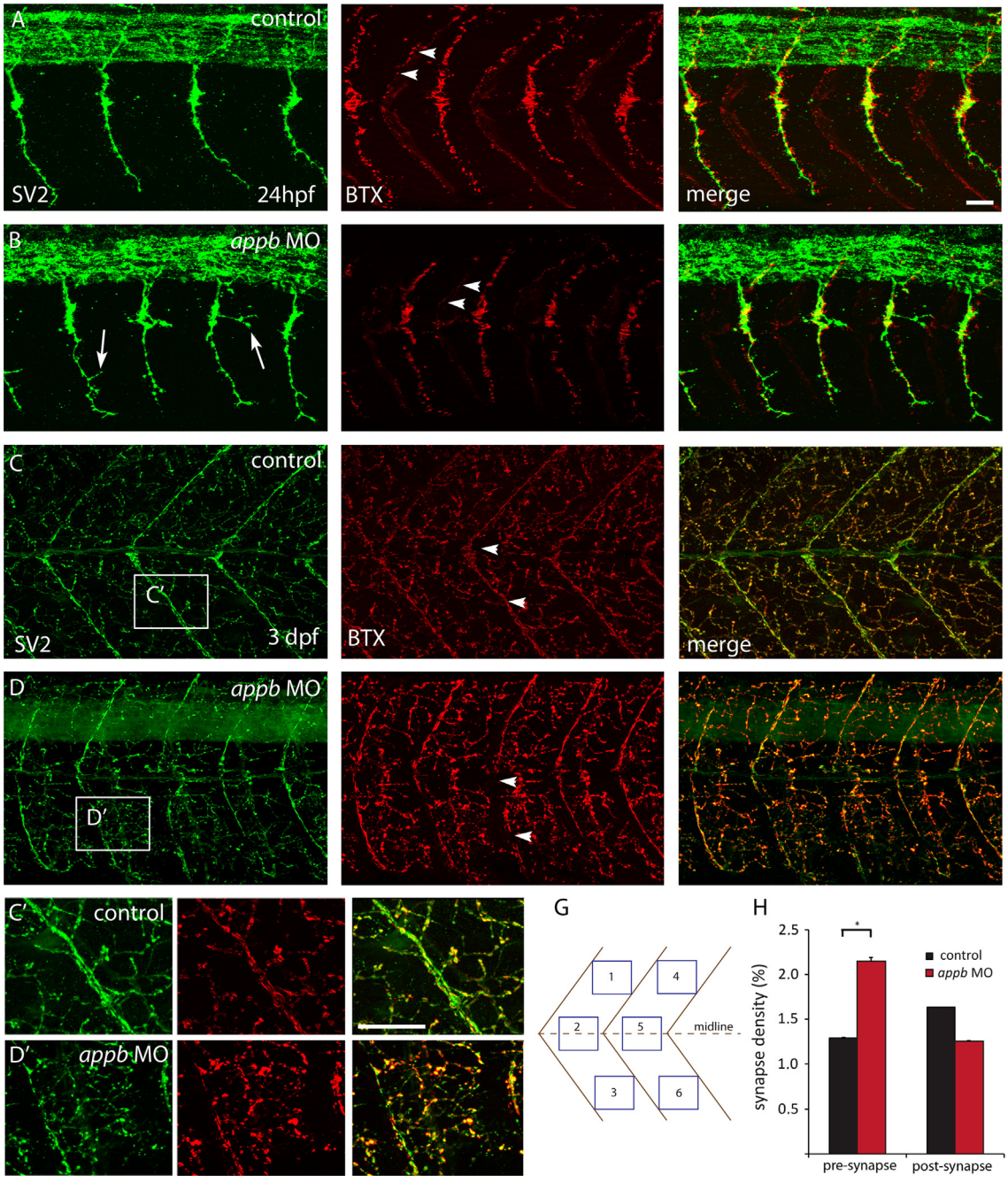

Fig. 8. Increased pre-synapses and decreased post-synapses. Neuromuscular synapses are labeled with antibodies against SV2 (green, pre-synaptic vesicles) and αBTX (red, post-synaptic AChRs). Images are oriented so that left is rostral and top is dorsal. At 24 hpf, PMN of wildtype embryos ($n=8$) extends straight axons projecting dorsally and ventrally has established robust and overlapping NMJs (A). In *appb* morphants ($n=8$,) the ventral projections are branched (arrows) and have less post-synapses at the horizontal myoseptum (arrowheads) compared to control (B). At 3 dpf there is an elaborative network of pre- and post-synapses. Control larvae have well defined NMJs at the horizontal myoseptum (arrowheads) and evenly distributed NMJs in the somites (C). The *appb* morphants (D) have interrupted synapse formation at the horizontal myoseptum (arrowheads) and at the midline. (C′, D′) Higher magnification of C and D. (H) Measurement of the density of pre- and post-synapses were made by counting 6 areas (G) distributed dorsally, ventrally or at the midline of two somites of each fish. Scale bars: A, C 20 μm.

The SMNs, forming shortly after the PMNs, are more reminiscent of motor neurons in other vertebrates including birds and mammals (Beattie et al., 1997). We show that the SMNs displayed a similar phenotype as the PMNs in that the ventrally projecting neurons are misguided when lowering the level of Appb. Although we cannot explain exactly how Appb affects the SMNs there are several possible alternatives. The motor neurons are guided by various cues in the surrounding tissue depending on their default migratory path. Although SMNs do not require PMNs for their outgrowth they follow the same path as PMNs if these are present (Pike et al., 1992). The mis-patterning of SMNs can therefore either be secondary to the excessive branching of the PMNs or caused by a direct effect of Appb reduction on the SMNs. The expression of *appb* by motor neurons suggests a cell autonomous requirement of Appb. Previous studies have suggested a role of APP in neurite growth and axonal guidance (Magara et al., 1999; Zheng et al., 1995) possibly through interaction with classic guidance cues such as semaphorin and netrin (Lourenco et al., 2009; Magdesian et al., 2011) or the DR6 receptor (Nikolaev et al., 2009). Our findings support a role for APP in the outgrowth and patterning of motor neurons. It is thus tempting to hypothesize

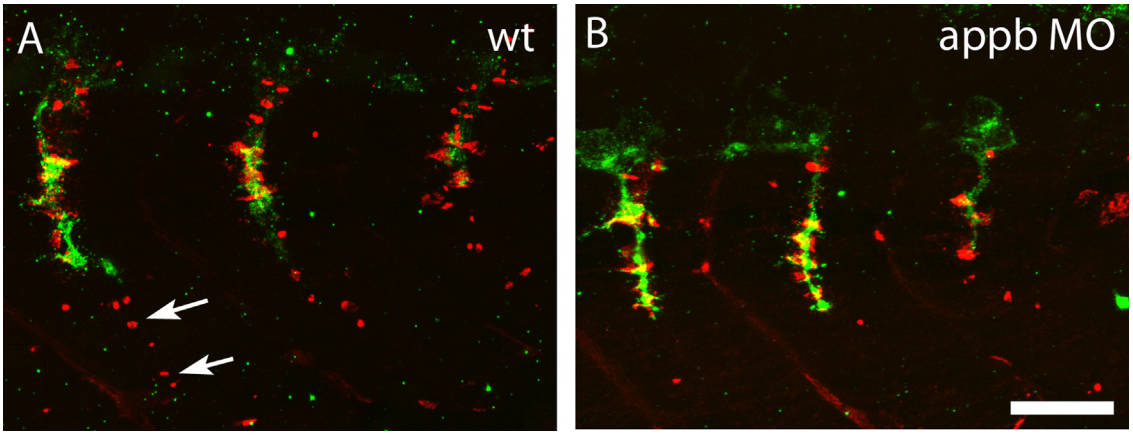

Fig. 9. Lack of pre-formed AChR clusters. Clusters of AChR in the muscle were stained with fluorescently labeled αBTX (red, post-synaptic AChRs) and projecting motor neurons stained with SV2 (green, pre-synaptic vesicles) antibody. At 28 hpf, pre-formed clusters containing AChR (arrows) were found dorsal to the migrating motor neuron tip in controls (A) while these were absent in *appb*MO injected embryos (B). Scale bar: 20 μm.

that Appb might interact with cues in the surrounding somite to guide motor neurons to the pre-patterned muscle targets. However, further studies are needed to provide evidence for such a mechanism.

Finally, reduction of Appb results in motor neurons with decreased ability to follow the predisposed pathway and embryos with elevated densities of pre-synapses and less post-synapses. This is in agreement with earlier studies showing that APP is required in both motor neurons and muscle to ensure the formation of functional NMJs (Wang et al., 2005). Here they showed that conditional knockout of *App* and *Aplp2* in muscle or motor neurons in mice resulted in increased pre-synaptic levels and decreased co-localization with post-synapses (Wang et al., 2005; Wang et al., 2009). In our study, muscle contractile tests showed normal muscle function but indicated hyper-excitability that would support an increased response to stimuli. However, we cannot conclude from these data whether it is an adverse structural synapse function or if it is the motor neuronal signal transmission that is the main cause for the observed locomotor abnormalities.

In conclusion, we show that Appb is important for the development and axogenesis of motor neurons in the spinal cord of the zebrafish, as well as for proper synapse formation at the NMJ. Reduced Appb levels result in behavioral defects including early hyperactivity and increased response to stimuli. The high conservation between fish and humans genes suggests that these functions may be conserved.

Acknowledgment

We thank Prof. P. Brehm for the use of the high-speed camera and supplying the Tg(*gata2:GFP*) fish and J. Sturve for providing the tracking system for behavior testing. We also thank Linda Werme and Malin Edling for the fish facility care. We acknowledge the Centre for Cellular Imaging at the Sahlgrenska Academy, University of Gothenburg for the use of imaging equipment and for the support from the staff. This study was funded by grants from the Swedish Research Council (projects KP2010-63P-21562-01-4 and K2011-61X-20401-05-6), the Wolfson Foundation, the Alzheimer's Association, Swedish State Support for Clinical Research (ALFGBG-144341), the Alzheimer Foundation, the Dementia Association, the Torsten and Ragnar Söderberg Foundation, the Swedish Brain Foundation (to P.K.), Stiftelsen för Gamla Tjänarinnor, and EU's Frame Project 7 (to P.K.).

Appendix A. Supporting information

Supplementary data associated with this article can be found in the online version at http://dx.doi.org/10.1016/j.ydbio.2013.06.026.

References

Allinquant, B., Hantraye, P., Mailleux, P., Moya, K., Bouillot, C., Prochiantz, A., 1995. Downregulation of amyloid precursor protein inhibits neurite outgrowth in vitro. J. Cell Biol. 128, 919–927.
Andermann, P., Ungos, J., Raible, D.W., 2002. Neurogenin1 defines zebrafish cranial sensory ganglia precursors. Dev. Biol. 251, 45–58.
Bateman, R.J., Xiong, C., Benzinger, T.L., Fagan, A.M., Goate, A., Fox, N.C., Marcus, D.S., Cairns, N.J., Xie, X., Blazey, T.M., Holtzman, D.M., Santacruz, A., Buckles, V., Oliver, A., Moulder, K., Aisen, P.S., Ghetti, B., Klunk, W.E., McDade, E., Martins, R. N., Masters, C.L., Mayeux, R., Ringman, J.M., Rossor, M.N., Schofield, P.R., Sperling, R.A., Salloway, S., Morris, J.C., 2012. Clinical and biomarker changes in dominantly inherited Alzheimer's disease. N. Engl. J. Med.
Beattie, C.E., 2000. Control of motor axon guidance in the zebrafish embryo. Brain Res. Bull. 53, 489–500.
Beattie, C.E., Hatta, K., Halpern, M.E., Liu, H., Eisen, J.S., Kimmel, C.B., 1997. Temporal separation in the specification of primary and secondary motoneurons in zebrafish. Dev. Biol. 187, 171–182.
Behra, M., Cousin, X., Bertrand, C., Vonesch, J.L., Biellmann, D., Chatonnet, A., Strahle, U., 2002. Acetylcholinesterase is required for neuronal and muscular development in the zebrafish embryo. Nat. Neurosci. 5, 111–118.
Berkowitz, A., Roberts, A., Soffe, S.R., 2010. Roles for multifunctional and specialized spinal interneurons during motor pattern generation in tadpoles, zebrafish larvae, and turtles. Front. Behav. Neurosci. 4, 36.
Blennow, K., de Leon, M.J., Zetterberg, H., 2006. Alzheimer's disease. Lancet 368, 387–403.
Brownstone, R.M., Bui, T.V., 2010. Spinal interneurons providing input to the final common path during locomotion. Prog. Brain Res. 187, 81–95.
Brustein, E., Saint-Amant, L., Buss, R.R., Chong, M., McDearmid, J.R., Drapeau, P., 2003. Steps during the development of the zebrafish locomotor network. J. Physiol. Paris 97, 77–86.
Buchhave, P., Minthon, L., Zetterberg, H., Wallin, A.K., Blennow, K., Hansson, O., 2012. Cerebrospinal fluid levels of beta-Amyloid 1–42, but not of Tau, are fully changed already 5 to 10 years before the onset of Alzheimer dementia. Arch. Gen. Psychiatry 69, 98–106.
Dawson, G.R., Seabrook, G.R., Zheng, H., Smith, D.W., Graham, S., O'Dowd, G., Bowery, B.J., Boyce, S., Trumbauer, M.E., Chen, H.Y., Van der Ploeg, L.H., Sirinathsinghji, D.J., 1999. Age-related cognitive deficits, impaired long-term potentiation and reduction in synaptic marker density in mice lacking the beta-amyloid precursor protein. Neuroscience 90, 1–13.
Devoto, S.H., Melancon, E., Eisen, J.S., Westerfield, M., 1996. Identification of separate slow and fast muscle precursor cells in vivo, prior to somite formation. Development (Cambridge, England) 122, 3371–3380.
Dou, Y., Andersson-Lendahl, M., Arner, A., 2008. Structure and function of skeletal muscle in zebrafish early larvae. J. Gen. Physiol. 131, 445–453.
Eisen, J.S., 1998. Genetic and molecular analyses of motoneuron development. Curr. Opin. Neurobiol. 8, 697–704.
Fetcho, J.R., Higashijima, S., McLean, D.L., 2008. Zebrafish and motor control over the last decade. Brain Res. Rev. 57, 86–93.
Flanagan-Steet, H., Fox, M.A., Meyer, D., Sanes, J.R., 2005. Neuromuscular synapses can form in vivo by incorporation of initially aneural postsynaptic specializations. Development (Cambridge, England) 132, 4471–4481.

Furutani-Seiki, M., Jiang, Y.J., Brand, M., Heisenberg, C.P., Houart, C., Beuchle, D., van Eeden, F.J., Granato, M., Haffter, P., Hammerschmidt, M., Kane, D.A., Kelsh, R.N., Mullins, M.C., Odenthal, J., Nusslein-Volhard, C., 1996. Neural degeneration mutants in the zebrafish, *Danio rerio*. Development (Cambridge, England) 123, 229–239.

Gabriel, J.P., Ausborn, J., Ampatzis, K., Mahmood, R., Eklof-Ljunggren, E., El Manira, A., 2011. Principles governing recruitment of motoneurons during swimming in zebrafish. Nat. Neurosci. 14, 93–99.

Goulding, M., 2009. Circuits controlling vertebrate locomotion: moving in a new direction. Nat. Rev. 10, 507–518.

Grillner, S., Jessell, T.M., 2009. Measured motion: searching for simplicity in spinal locomotor networks. Curr. Opin. Neurobiol. 19, 572–586.

Heber, S., Herms, J., Gajic, V., Hainfellner, J., Aguzzi, A., Rulicke, T., von Kretzschmar, H., von Koch, C., Sisodia, S., Tremml, P., Lipp, H.P., Wolfer, D.P., Muller, U., 2000. Mice with combined gene knock-outs reveal essential and partially redundant functions of amyloid precursor protein family members. J. Neurosci. 20, 7951–7963.

Higashijima, S., Hotta, Y., Okamoto, H., 2000. Visualization of cranial motor neurons in live transgenic zebrafish expressing green fluorescent protein under the control of the islet-1 promoter/enhancer. J. Neurosci. 20, 206–218.

Hirata, H., Carta, E., Yamanaka, I., Harvey, R.J., Kuwada, J.Y., 2009. Defective glycinergic synaptic transmission in zebrafish motility mutants. Front. Mol. Neurosci. 2, 26.

Holcomb, L.A., Gordon, M.N., Jantzen, P., Hsiao, K., Duff, K., Morgan, D., 1999. Behavioral changes in transgenic mice expressing both amyloid precursor protein and presenilin-1 mutations: lack of association with amyloid deposits. Behav. Genet. 29, 177–185.

Ikin, A.F., Sabo, S.L., Lanier, L.M., Buxbaum, J.D., 2007. A macromolecular complex involving the amyloid precursor protein (APP) and the cytosolic adapter FE65 is a negative regulator of axon branching. Mol. Cell. Neurosci. 35, 57–63.

Jacobsen, K.T., Iverfeldt, K., 2009. Amyloid precursor protein and its homologues: a family of proteolysis-dependent receptors. Cell Mol. Life Sci. 66, 2299–2318.

Jin, L.W., Ninomiya, H., Roch, J.M., Schubert, D., Masliah, E., Otero, D.A., Saitoh, T., 1994. Peptides containing the RERMS sequence of amyloid beta/A4 protein precursor bind cell surface and promote neurite extension. J. Neurosci. 14, 5461–5470.

Joshi, P., Liang, J.O., Dimonte, K., Sullivan, J., Pimplikar, S.W., 2009. Amyloid precursor protein is required for convergent-extension movements during Zebrafish development. Dev. Biol.

Kim, C., Srivastava, S., Rice, M., Godenschwege, T.A., Bentley, B., Ravi, S., Shao, S., Woodard, C.T., Schwartz, L.M., 2011. Expression of human amyloid precursor protein in the skeletal muscles of Drosophila results in age- and activity-dependent muscle weakness. BMC Physiol. 11, 7.

Kucenas, S., Wang, W.D., Knapik, E.W., Appel, B., 2009. A selective glial barrier at motor axon exit points prevents oligodendrocyte migration from the spinal cord. J. Neurosci. 29, 15187–15194.

Lalonde, R., Fukuchi, K., Strazielle, C., 2012. Neurologic and motor dysfunctions in APP transgenic mice. Rev. Neurosci. 23, 363–379.

LeBlanc, A.C., Kovacs, D.M., Chen, H.Y., Villare, F., Tykocinski, M., Autilio-Gambetti, L., Gambetti, P., 1992. Role of amyloid precursor protein (APP): study with antisense transfection of human neuroblastoma cells. J. Neurosci. Res. 31, 635–645.

Lourenco, F.C., Galvan, V., Fombonne, J., Corset, V., Llambi, F., Muller, U., Bredesen, D.E., Mehlen, P., 2009. Netrin-1 interacts with amyloid precursor protein and regulates amyloid-beta production. Cell Death Differ. 16, 655–663.

Magara, F., Muller, U., Li, Z.W., Lipp, H.P., Weissmann, C., Stagljar, M., Wolfer, D.P., 1999. Genetic background changes the pattern of forebrain commissure defects in transgenic mice underexpressing the beta-amyloid-precursor protein. Proc. Natl. Acad. Sci. U.S.A 96, 4656–4661.

Magdesian, M.H., Gralle, M., Guerreiro, L.H., Beltrao, P.J., Carvalho, M.M., Santos, L.E., de Mello, F.G., Reis, R.A., Ferreira, S.T., 2011. Secreted human amyloid precursor protein binds semaphorin 3a and prevents semaphorin-induced growth cone collapse. PLoS One 6, e22857.

McGraw, H.F., Nechiporuk, A., Raible, D.W., 2008. Zebrafish dorsal root ganglia neural precursor cells adopt a glial fate in the absence of neurogenin1. J. Neurosci. 28, 12558–12569.

Meng, A., Tang, H., Ong, B.A., Farrell, M.J., Lin, S., 1997. Promoter analysis in living zebrafish embryos identifies a cis-acting motif required for neuronal expression of GATA-2. Proc. Natl. Acad. Sci. U.S.A 94, 6267–6272.

Milner, L.D., Landmesser, L.T., 1999. Cholinergic and GABAergic inputs drive patterned spontaneous motoneuron activity before target contact. J. Neurosci. 19, 3007–3022.

Milward, E.A., Papadopoulos, R., Fuller, S.J., Moir, R.D., Small, D., Beyreuther, K., Masters, C.L., 1992. The amyloid protein precursor of Alzheimer's disease is a mediator of the effects of nerve growth factor on neurite outgrowth. Neuron 9, 129–137.

Musa, A., Lehrach, H., Russo, V.A., 2001. Distinct expression patterns of two zebrafish homologues of the human APP gene during embryonic development. Dev. Genes Evol. 211, 563–567.

Myers, P.Z., 1985. Spinal motoneurons of the larval zebrafish. J Comp Neurol 236, 555–561.

Myers, P.Z., Eisen, J.S., Westerfield, M., 1986. Development and axonal outgrowth of identified motoneurons in the zebrafish. J. Neurosci. 6, 2278–2289.

Nikolaev, A., McLaughlin, T., O'Leary, D.D., Tessier-Lavigne, M., 2009. APP binds DR6 to trigger axon pruning and neuron death via distinct caspases. Nature 457, 981–989.

Panzer, J.A., Gibbs, S.M., Dosch, R., Wagner, D., Mullins, M.C., Granato, M., Balice-Gordon, R.J., 2005. Neuromuscular synaptogenesis in wild-type and mutant zebrafish. Dev. Biol. 258, 340–357.

Paquet, D., Bhat, R., Sydow, A., Mandelkow, E.M., Berg, S., Hellberg, S., Falting, J., Distel, M., Koster, R.W., Schmid, B., Haass, C., 2009. A zebrafish model of tauopathy allows in vivo imaging of neuronal cell death and drug evaluation. J. Clin. Invest. 119, 1382–1395.

Perez, R.G., Zheng, H., Van der Ploeg, L.H., Koo, E.H., 1997. The beta-amyloid precursor protein of Alzheimer's disease enhances neuron viability and modulates neuronal polarity. J. Neurosci. 17, 9407–9414.

Pike, S.H., Melancon, E.F., Eisen, J.S., 1992. Pathfinding by zebrafish motoneurons in the absence of normal pioneer axons. Development (Cambridge, England) 114, 825–831.

Pozueta, J., Lefort, R., Shelanski, M.L., 2012. Synaptic changes in Alzheimer's disease and its models. Neuroscience.

Saint-Amant, L., Drapeau, P., 1998. Time course of the development of motor behaviors in the zebrafish embryo. J. Neurobiol. 37, 622–632.

Sanes, J.R., Lichtman, J.W., 1999. Development of the vertebrate neuromuscular junction. Annu. Rev. Neurosci. 22, 389–442.

Seo, J.S., Leem, Y.H., Lee, K.W., Kim, S.W., Lee, J.K., Han, P.L., 2010. Severe motor neuron degeneration in the spinal cord of the Tg2576 mouse model of Alzheimer disease. J. Alzheimer's Dis. 21, 263–276.

Small, D.H., Nurcombe, V., Reed, G., Clarris, H., Moir, R., Beyreuther, K., Masters, C.L., 1994. A heparin-binding domain in the amyloid protein precursor of Alzheimer's disease is involved in the regulation of neurite outgrowth. J. Neurosci. 14, 2117–2127.

Song, P., Pimplikar, S.W., 2012. Knockdown of amyloid precursor protein in zebrafish causes defects in motor axon outgrowth. PLoS One 7, e34209.

Stemple, D.L., Solnica-Krezel, L., Zwartkruis, F., Neuhauss, S.C., Schier, A.F., Malicki, J., Stainier, D.Y., Abdelilah, S., Rangini, Z., Mountcastle-Shah, E., Driever, W., 1996. Mutations affecting development of the notochord in zebrafish. Development (Cambridge, England) 123, 117–128.

Teraoka, H., Urakawa, S., Nanba, S., Nagai, Y., Dong, W., Imagawa, T., Tanguay, R.L., Svoboda, K., Handley-Goldstone, H.M., Stegeman, J.J., Hiraga, T., 2006. Muscular contractions in the zebrafish embryo are necessary to reveal thiuram-induced notochord distortions. Toxicol. Appl. Pharmacol. 212, 24–34.

Wang, P., Yang, G., Mosier, D.R., Chang, P., Zaidi, T., Gong, Y.D., Zhao, N.M., Dominguez, B., Lee, K.F., Gan, W.B., Zheng, H., 2005. Defective neuromuscular synapses in mice lacking amyloid precursor protein (APP) and APP-Like protein 2. J. Neurosci. 25, 1219–1225.

Wang, Z., Wang, B., Yang, L., Guo, Q., Aithmitti, N., Songyang, Z., Zheng, H., 2009. Presynaptic and postsynaptic interaction of the amyloid precursor protein promotes peripheral and central synaptogenesis. J. Neurosci. 29, 10788–10801.

Westerfield, M., Eisen, J.S., 1988. Neuromuscular specificity: pathfinding by identified motor growth cones in a vertebrate embryo. Trends Neurosci. 11, 18–22.

Westerfield, M., McMurray, J.V., Eisen, J.S., 1986. Identified motoneurons and their innervation of axial muscles in the zebrafish. J. Neurosci. 6, 2267–2277.

Young-Pearse, T.L., Bai, J., Chang, R., Zheng, J.B., LoTurco, J.J., Selkoe, D.J., 2007. A critical function for beta-amyloid precursor protein in neuronal migration revealed by in utero RNA interference. J. Neurosci. 27, 14459–14469.

Zeller, J., Schneider, V., Malayaman, S., Higashijima, S., Okamoto, H., Gui, J., Lin, S., Granato, M., 2002. Migration of zebrafish spinal motor nerves into the periphery requires multiple myotome-derived cues. Dev. Biol. 252, 241–256.

Zheng, H., Jiang, M., Trumbauer, M.E., Sirinathsinghji, D.J., Hopkins, R., Smith, D.W., Heavens, R.P., Dawson, G.R., Boyce, S., Conner, M.W., Stevens, K.A., Slunt, H.H., Sisoda, S.S., Chen, H.Y., Van der Ploeg, L.H., 1995. beta-Amyloid precursor protein-deficient mice show reactive gliosis and decreased locomotor activity. Cell 81, 525–531.